

SPECIFICS OF MECHANICALLY DRIVEN ATOMIC DISTRIBUTIONS IN INTERSTITIAL ALLOYS

Jacques Foct^ξ

Laboratoire de Métallurgie Physique et Génie des Matériaux – UMR CNRS 8517 – Université de Lille, France

Keywords: Ball milling, Fe-N Fe-C alloys, Interstitial distributions, Nanostructure, Mössbauer spectroscopy, Inverse Hall Petch behaviour

Abstract

Mechanically driven interstitial atoms distributions are exemplified in the case of FeI_x (I = C or N) alloys obtained by ball milling process in the concentration range 0.05 ≤ x ≤ 0.5. With the chosen processing protocol, the asymptotic completion interstitial distribution depends on x and on the nature of interstitial (C or N) and not on the reactants which only have to respect the aimed nominal composition of the mixture. Mössbauer spectrometry results have proven that the distribution observed for similar interstitial compositions for C and for N are different. The grounds of these differences and the consequences on the structure of mechanically driven alloys are analysed, as well as the influence of nano-structuration on plasticity nano-mechanisms. The role of stacking faults shown by diffraction and microscopy results as well as other lattice defects and phase transformation is examined.

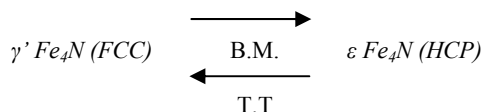
Introduction

Mechanically driven atomic distributions in solid state alloys may result from different phenomena or processes such as neutron irradiation, severe plastic deformation (S.P.D.), ball milling (B.M.), wear, friction, fatigue and impact, meanwhile strain-stress rate induced redistribution may also result from very usual fabrication processes such as more or less soft loading specially in interstitial alloys of transition elements such as Fe. Because the final structure results from chemical and from mechanical phenomena, the interpretation of this processing may often be confused. In the case of neutron irradiation, such as atomic cascades which takes place in the vessel steel of a nuclear power reactor, the contributions of ballistic and atomic potential parameters can be taken into account, thanks to molecular dynamics and Monte Carlo simulations, during very short period of time. In contrast with this case, S.P.D. and B.M. induced atomic redistributions, alloying reactions and phases transformations are still a matter of debate mainly because : (1) the atomic displacements take place at several locations of the crystalline grains ; (2) are involved lattice defects such as vacancies, dislocations, stacking faults, twins, grain and phase boundaries ; (3) all the quoted phenomena interfere during all the lasting process (several hours); (4) relaxation and thermally activated ageing processes are pulling the highly metastable configuration back towards equilibrium state. For the present study, the similarities of C and N atoms interactions with lattice defects and their comparable diffusion coefficients suggested that mechanisms resulting from purely mechanical phenomena could be considered in FeC_x and FeN_x as similar and that the observed differences would mainly result from physicochemical parameters

controlled by the I-I and Fe-I interactions. Since about 30 years, Mössbauer effect (M.E.) has been proven to provide a privileged technique for studying assemblies of nanosized particles and nanostructured materials as commented in sound review such as [1-2]. In comparison with the study of B.M. induced phenomena in substitutional alloys, the case of interstitials offers many advantages : the diffusion C and N is quasi independent of lattice defects – the fast migration of interstitial atoms originates B.M. reaction kinetics which reduce the time of completion at least by one or two orders of magnitude - binary FeC_x and FeN_x are showing magnetic coupling in a large x interval and the electronic interactions between interstitials and Fe lead to distinguish the different neighbourhood by Mössbauer spectroscopy. Another advantage provided by the important Fe-C, Fe-N, C-C, N-N interactions results from the formation of well defined equilibrium interstitial distributions and compounds which are likely to constitute actual ordering references for the calibration of experimental results. Even if the above underlined points about mechanically driven iron based interstitial alloys have not been always explicitly commented, numerous articles devoted to this subject demonstrated its interest. Albeit binary FeN_x alloys, for x > 0,25 %, are unstable under atmospheric pressure because chemical potential of N in the solid phase is much higher than in the gas, milling of highly concentrated compounds has been proven to take place without appreciable loss of nitrogen and the following mechano-chemistry equation has been established [3] :



Thanks to this conservation equation, results obtained on B.M. FeN_x alloys can be compared to B.M. FeC_x compounds obtained either from graphite or from iron carbides and Fe precursors [4]. It has been shown that phase transformations are induced by ball milling and this not only under high energetic conditions but even through crunching interstitial samples such as γ' Fe₄N or θ Fe₃C in a mortar [5]. When γ' Fe₄N is submitted to B.M. at less than 2 hours the initial Perovskite-like cubic structure is transformed into a hexagonal ε-like structure. A thermal treatment (T.T.) at 200°C, restores the thermodynamically stable γ' phase [3].



Besides the interest of carbides, nitrides and carbonitrides as model materials for the interpretation of mechano-chemistry phenomena, the important applications of these ball-milled

^ξ email : jacques.foct@univ-lille1.fr

compounds in powder metallurgy, surface treatment, tribology, wear resistance and thermal barrier should not be omitted.

X-Ray diffraction measurements achieved by Aufrecht *et al* [6] on well defined BM Fe-N powders have shown that the micro-strain versus grain size variation is not monotonous but presents a maximum near 10 nm, a value which could correspond to the transition from the deformation mechanism of ultra fine grain to that taking place in actual nano-grains. The identification of this frontier may contribute to define an optimal grain size window for industrial application and to a pertinent choice to develop severe plastic deformation process.

Experimental and Results

B.M. reactions have been achieved in a high energy vibratory mill (SPEX 8000) with a constant ball to powder ratio of 10:1 [5]. A rather classical protocol has been chosen: series of periodic 1 hour milling interrupted by ½ hour cooling rest aimed to reduce the inconvenience of the heating of vial and balls. In contrast with B.M. reactions of substitutional alloys, the rather fast kinetics allowed limiting the actual milling duration to 32 hours and the final products were compared with intermediate 16 hours products. In order to avoid or at least to minimize, any oxidation reaction the filling of the vial was made under argon atmosphere and the vial was never open before the final achievement. Milling of FeC_x alloys was achieved from Fe₃C (CERAC, 45 μm) + Fe (GOODFELLOW, 60 μm) and graphite (< 60 μm) + Fe powders. Nitrogen source was ζ Fe₂N synthesised by Fe-NH₃ solid – gas reaction (450 °C - 8 hours, gas flow 0,175 l/min). The following target compositions corresponding to Fe₈C, Fe₃C, Fe₂C and Fe₈N, Fe₄N, Fe₃N were suggested by “virtual” as well as actual stoichiometric ordering under equilibrium conditions. Previous experiments, under the same protocol, have shown that when the contamination from the experimental device (steel of balls and vial) is reduced by previous “white” test millings the nominal composition can be considered as significant and that the difference with chemical analysis is less than 5 at % [6]. The characteristics of the as-milled powder are given on Table 1.

Table 1. Processing parameters and nominal compositions of samples

Fe-C System			Fe-N System		
Final Alloys	Initial Powders	Time (h)	Final Alloys	Initial Powders	Time (h)
Fe ₈ C-16	8 Fe + Cgr	16	Fe ₈ N-16	6 Fe + ζ Fe ₂ N	16
Fe ₈ C-32	8 Fe + Cgr	32	Fe ₈ N-32	6 Fe + ζ Fe ₂ N	32
Fe ₈ C'-16	5 Fe + Fe ₃ C	16	Fe ₈ N'-16	5.17 Fe + ε Fe _{2.83} N	16
Fe ₈ C'-32	5 Fe + Fe ₃ C	32	Fe ₈ N'-32	5.17 Fe + ε Fe _{2.83} N	32
-	-	-	Fe ₄ N-16	2 Fe + ζ Fe ₂ N	16
-	-	-	Fe ₄ N-32	2 Fe + ζ Fe ₂ N	32
Fe ₃ C-16	3 Fe + Cgr	16	Fe ₃ N-16	Fe + ζ Fe ₂ N	16
Fe ₃ C-32	3 Fe + Cgr	32	Fe ₃ N-32	Fe + ζ Fe ₂ N	32
Fe ₂ C-16	2 Fe + Cgr	16	-	-	-
Fe ₂ C-32	2 Fe + Cgr	32	-	-	-

In addition to the intrinsic complexity of the structure of B.M. products and of the phenomena involved during the processing, contamination constitutes a recurrent obstacle to obtain unambiguous characterization of the B.M. powders. Because the single-versus multi-phase feature of the product as well as the composition homogeneity result from very small scale (~ nm) fluctuations they are often masked in electronic microprobe analysis and a fortiori in global chemical analysis; therefore, characterization demands different techniques such as X-Ray and electron diffraction, electronic as well as nuclear spectroscopy, atomic probe analysis, transmission electron microscopy (T.E.M.). In interstitial alloys the occupation rate of interstitial sites plays a key role, although the available amount of sites depends on their nature (tetrahedral, octahedral and prismatic sites) and of the crystallographic structure the parameter x, defined by formula FeI_x is considered here because x may be deduced from Mössbauer spectra.

Table 2. Hyperfine Field (H in Tesla) and Relative Abundances (A in %) of Fe₈C, Fe₈N, Fe₃C and Fe₄N after 16 and 32 hours ball milling.

Fe-C system			Fe-N system			Fe-C system			Fe-N system		
Alloys	H (T)	A (%)									
Fe ₈ C-16	34.19	6.3	Fe ₈ N-16	35.31	8.1	Fe ₃ C-16	33.12	3.6	Fe ₄ N-16	34.73	7.4
	33.00	23.4		33.03	44.9		24.91	10.6		33.22	28.7
	30.07	3.9		30.27	14.1		20.95	37.1		29.88	18.6
	27.55	5.3		27.45	9.3		20.91	20.8		27.55	14.8
	24.35	7.4		-	5.8		18.37	22.0		23.67	18.5
	19.98	39.4		-	8.1		-	5.9		-	4.6
	-	14.3		-	8.7		-			-	7.4
		-	1								
Fe ₈ C-32	34.46	8.5	Fe ₈ N-32	35.00	9.1	Fe ₃ C-32	30.77	3.7	Fe ₄ N-32	34.87	3.9
	33.00	34.8		33.20	41.2		25.20	10.3		32.82	17.4
	30.46	4.2		30.25	15.9		20.69	42.6		28.82	20.1
	27.55	5.7		27.53	13.0		20.69	43.4		26.18	20.6
	23.86	5.7		-	4.6					21.49	23.3
	19.69	27.5		-	8.9					-	10.4
	-	13.6		-	5.4					-	4.3
		-	1.9								

Mössbauer spectra have been obtained, at room temperature, with a Wissel MR-300 constant acceleration driving unit and DFG-1200 digital function generator, in the $\pm 8 \text{ mm s}^{-1}$ range. The 1 GBq ^{57}Co source is dissolved in a Rhodium matrix. The calibration of velocity refers to $\alpha\text{-Fe}$ spectrum. The study of the spectra corresponding to all products of Table 1 has shown that the main features are exemplified by spectra corresponding to Fe_8C , Fe_8N , Fe_3C and Fe_4N milled 16 and 32 hours (Fig. 1 and

Fig. 2). The larger fluctuation of hyperfine parameters in B.M. nitrogen compounds than in corresponding carbon products (Table 2) and the X-Ray diffraction (XRD) pattern (X'Pert Pro diffractometer, $\lambda_{\text{Co}} = 0.179021 \text{ nm}$) showing much broader diffraction peaks for FeN_x than for FeC_x suggest a more heterogeneous distribution of N than of C which will be discussed here after.

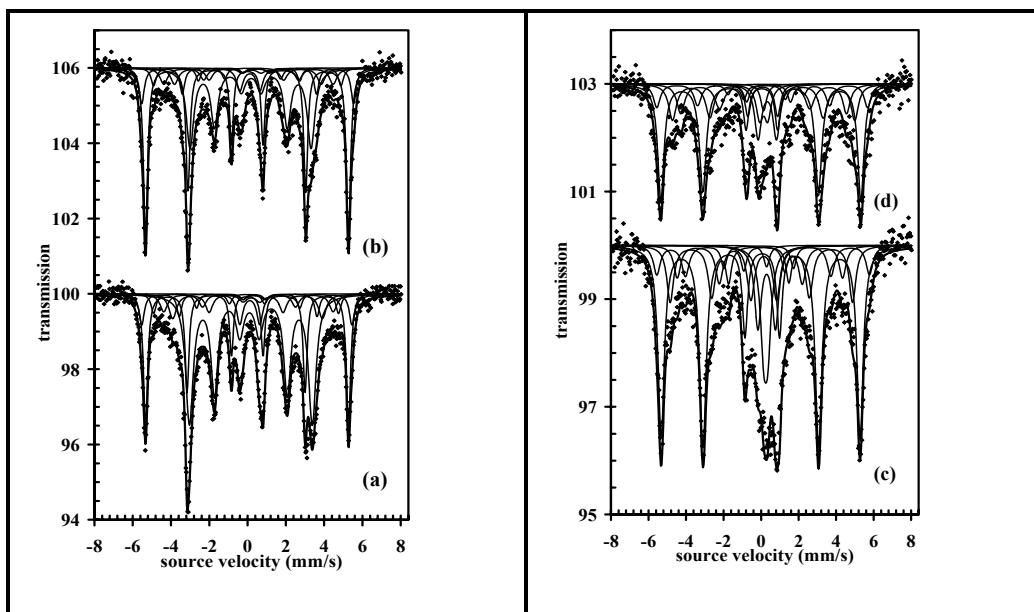


Figure 1. Mössbauer spectra and computer deconvolutions - (a) $8\text{Fe}+\text{C}_{\text{gr}} \rightarrow \text{Fe}_8\text{C}$ 16h MA; (b) $8\text{Fe}+\text{C}_{\text{gr}} \rightarrow \text{Fe}_8\text{C}$ 32h MA; (c) $6\text{Fe}+\zeta\text{Fe}_2\text{N} \rightarrow \text{Fe}_8\text{N}$ 16h MA; (d) $6\text{Fe}+\zeta\text{Fe}_2\text{N} \rightarrow \text{Fe}_8\text{N}$ 32h MA

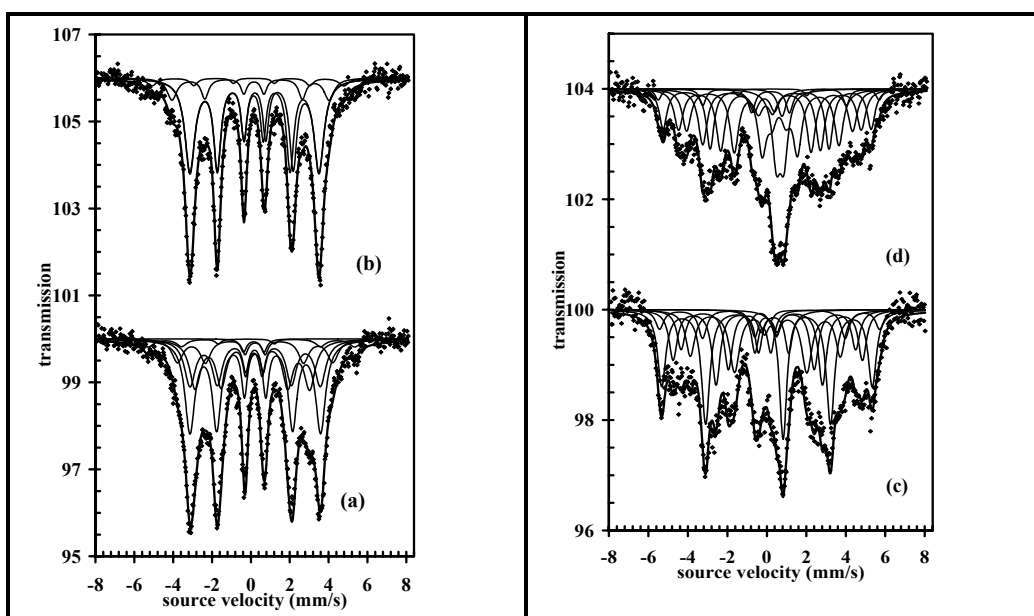


Figure 2. Mössbauer spectra and computer deconvolutions (a) $3\text{Fe}+\text{C}_{\text{gr}} \rightarrow \text{Fe}_3\text{C}$ 16 h MA; (b) $3\text{Fe}+\text{C}_{\text{gr}} \rightarrow \text{Fe}_3\text{C}$ 32 h MA; (c) $2\text{Fe}+\zeta\text{Fe}_2\text{N} \rightarrow \text{Fe}_4\text{N}$ 16 h MA; (d) $2\text{Fe}+\zeta\text{Fe}_2\text{N} \rightarrow \text{Fe}_4\text{N}$ 32 h MA

Discussion

Ball milling of FeN_x with $x = 0.125$, corresponding to Fe_8N , has been stimulated by the promising magnetic properties of $\alpha''\text{Fe}_8\text{N}$ obtained by precipitation in N supersaturated α ferrite [7] as well as by ageing of $\alpha'\text{FeN}_x$ martensite [3, 7] and of ϵFeN_x [8]. XRD characterisation of B.M. FeN_x appeared difficult, diffraction peaks after milling are broad, non symmetrical and become extremely imprecise as soon as the order of reflection increase. This results from size and stress effects, atomic disorder and composition fluctuations. Only very sophisticated deconvolutions of carefully obtained diffractograms are likely to avoid ambiguous interpretations. In the case of FeN_x this deconvolution achieved by Aufrecht *et al* [6] has proven that for $x \leq 0.14$ the martensitic-like tetragonal structure which had been proposed [9] does not satisfy all the experimental diffraction data and that the α'' superferritic BCC suggested by Mössbauer spectroscopy [10] and electron diffraction is more realistic [11]. Arguments in favour of α'' -like structure were also provided by 200°C ageing of the B.M. products which in contrast with similar thermal treatment of as-quenched α' martensite refused any evidence of $\alpha''\text{Fe}_{16}\text{N}_2$ ordering [12]. Curiously, it seems that the most convenient arguments in favour of a B.M. induced α' martensite-like structure had never been proposed by the authors who concluded to its actuality: an α' type distribution would result from a B.M. induced shear transformation of a FCC γ or HCP ϵ mother phase for which only one octahedral site per iron atom is available. According to this hypothesis a transient γ or ϵ phase should be detected. Although the presence of the very small amount of FCC phase identified by Aufrecht *et al* [6] may show that the role of a transient amount of austenite can not be completely excluded, a B.M. mechanism likely to induce the formation as well as the martensitic collapse of austenite may be masked by the important thermal redistribution of interstitials. Therefore, the main source of controversy probably arises from the difference in the experimental conditions (ball diameter and weight, vessel volume and dimensions, ageing temperature) which may dramatically change the evolution of the ball milling product during the ageing period. As long as complete diffraction analyses of the here obtained powders, for $x > 0.125$, have not been achieved comparison between FeC_x and FeN_x is mainly based on Mössbauer spectra. Thanks to many experimental measurements in different iron interstitial alloys, hyperfine fields ($H(i)$), at the iron nucleus, obey a quasi linear dependence versus the number of interstitial nearest neighbours [13] at least for 0, 1, 2 and sometime 3 neighbours. It is therefore possible to associate environments Fe_i (i = number of I nnn) to the following H intervals: Fe_0 ($H > 32\text{T}$), Fe_1 ($32\text{T} > H > 27\text{T}$), Fe_2 ($25\text{T} > H > 18\text{T}$), Fe_3 (paramagnetic or $H < 18\text{T}$).

Despite the uncertainties concerning $H(i)$ function, mainly correlated with first nearest neighbouring, which neglects the influence of second nearest neighbours as well as of the interstitial site distortion, unambiguous remarks are deduced:

1. The faint variation of the H values, between 16 and 32 B.M. hours, shows that the present protocol leads to a steady mechano-chemical state and as already underlined not of the reactants;
2. The deconvolution of spectra corresponding to Fe_8I showed that, when $I = \text{C}$ or N , hyperfine field H_0 and H_1

do not strongly depend on the nature of the interstitial in contrast with the observed larger decrease of H induced by N than by C when $i \geq 2$. The important decrease of H induced by N , when $i \geq 2$, could be considered as an argument for an electron donor role of the interstitials (rigid d band approximation, decreasing stability of transition metals carbides and nitrides with the d electrons filling) which is consistent with ab-initio calculations [14-15];

3. Mössbauer peaks corresponding to paramagnetic and, in some cases superparamagnetic environments, clearly more frequent in nitrogen than in carbon B.M. alloys are not only related with the previous remark but also with the thermal stability of the alloys. These environments are not stable in α'' and ϵ like FeN_x phases and generate nitrogen enriched pre-precipitates zones (Fig. 1 and Fig. 2);
4. In presence of carbon, hyperfine parameters of B.M. Fe_3C Mössbauer environments are close to those measured in well crystallized $\theta\text{Fe}_3\text{C}$ and $\chi\text{Fe}_5\text{C}_2$. Fe_7C_3 [16-17]. In similar conditions, with nitrogen, B.M. Fe_4N Mössbauer environments are comparable with those of ϵFeN_x and ζFeN_x phases. In both cases the B.M. destruction of perfect structures is likely to result from a stacking fault based mechanism. A FCC \rightarrow HCP B.M. mechanism operating in Fe_4N does not destroy the octahedral interstitial site but changes the inter-sites relations. In FeC_x ($0.15 \leq x \leq 0.5$) the corrugated -like structure of carbides, characterized by sheets of trigonal interstitial prismatic sites, is partially disordered under milling; Fe_i iron atoms are yet vertices shared by one empty octahedron and i occupied trigonal prisms ;
5. Mössbauer spectroscopy as well as ab initio calculations show that interaction potential between C and C , N and N , C and N are different and responsible of dramatically different distributions and re-distributions of interstitial atoms when the metallic composition is maintained constant. Therefore the design of new steel grades alloyed with more than one interstitial species should open promising solutions to reach higher properties.
6. The possibility demonstrated by Aufrecht *et al* [6] to accurately measure the characteristic length of the nano-structure controlled by the N concentration shows that when this length becomes close to or lower than 10 nm the deformation mechanism changes from dislocations pile-up to grain boundary sliding-like.
7. The identity of BM products obtained from single phase primers and multi-phases mixtures does not contradict the model formerly proposed [3] in the case of interstitial alloys.

Despite the complexity of Mössbauer spectra, similar environments are determined for different nitrogen content. That the abundances neither obey a binominal distribution nor an ordered one shows that the N-N interactions are important but not large enough to restore a martensitic like order α' or α'' . Therefore, it is proposed that the distribution resulting from ball-

milling is a hybridization of martensitic (α' and α'') and ferritic (α , α''') distribution. In both cases N atoms occupy octahedral sites, ab-initio calculations (14,15) showed that the tetrahedral position is unstable, the hypothesis of an appreciable (much larger than necessary to N diffusion) occupation of tetrahedra is excluded.

An interstitial order vector $\vec{\Omega}$ can be defined by the amount of N interstitials occupying the different dipolar octahedral sites for which the four fold symmetry axes are the three references axes.

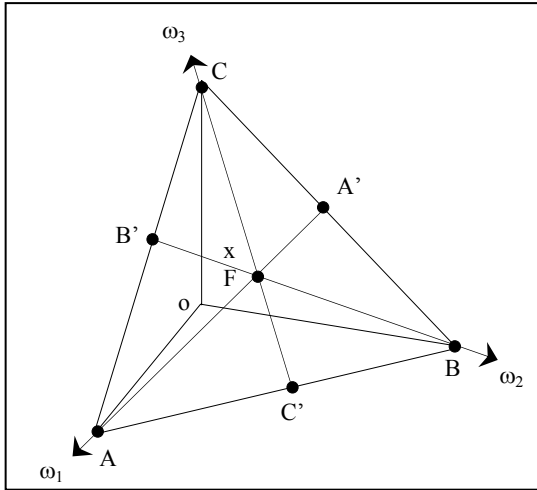
$$(\vec{\Omega}) = \begin{pmatrix} \omega_1 \\ \omega_2 \\ \omega_3 \end{pmatrix} \quad (1)$$

In FeN_x the following constraint is obeyed :

$$\omega_1 + \omega_2 + \omega_3 = x \quad (2)$$

Relation (2) corresponds to an octahedral plane in the orthogonal reference frame of $\vec{\Omega}$. Points of the equilateral triangle defined the interstitial distribution. The center F correspond to ferritic BCC ordering α or α''' ($\omega_1 = \omega_2 = \omega_3 = \frac{x}{3}$). The vertices A,B,C. correspond to bct “perfect” α'

martensite with $\frac{e}{a} > 1$.



Middles of AB, BC, CA also corresponds to a bct lattice with $\frac{c}{a} < 1$. All points which are not close to A, B, C, A', B', C', and F correspond to lattices which show orthorhombic symmetry.

The lattice distortion originated by interstitial distribution $\vec{\Omega}$ characteristic of a domain of which the length scale is Λ can be approximate by :

$$\begin{aligned} a_1 &= a_0 + \alpha \omega_1 - \beta \omega_2 - \beta \omega_3 \\ a_2 &= a_0 - \beta \omega_1 + \alpha \omega_2 - \beta \omega_3 \\ a_3 &= a_0 - \beta \omega_1 - \beta \omega_2 + \alpha \omega_3 \end{aligned} \quad (3)$$

Which can be written

$$(a) = (a_0) + (\alpha_{ij}) (\vec{\Omega})$$

(a), (a_0) and (Ω) are column matrices.

(α_{ij}) is a 3 x 3 matrix $a_{ii} = \alpha$

$$a_{ij} = -\beta$$

α and β can be deduced from lattice parameter measurements on α' martensite.

In addition to the influence of the distortion of the lattice resulting from the N interstitial atoms distribution, the X-ray diffraction pattern depends on the size of the diffraction domains Λ , on the length scale of the concentration fluctuation, on the internal strains, on the texture.

The present discussion is emphasizing the role of lattice distortion induced by the interstitial distribution. The order vector $\vec{\Omega}$ in the frame $\vec{\omega}_1, \vec{\omega}_2, \vec{\omega}_3$ is defined over a crystalline domain λ of some cells ($\lambda \sim$ some nm) is $\vec{\Omega}$ is a function of the coordinates of the domain under consideration $\vec{\Omega}(\vec{X})$. Coordinate of \vec{X} refer to the specimen space frame $\vec{\chi}_1, \vec{\chi}_2, \vec{\chi}_3$.

The idea is to propose a statistical distribution of $\vec{\Omega}$ likely to be consistent with the description suggested by Mössbauer spectroscopy on the one hand and on the other hand to be consistent with the diffraction pattern. The average nitrogen concentration in the domain λ^3 around \vec{X} is $\bar{X}(\vec{x})$ and the corresponding equilateral triangle of possible $\vec{\Omega}$ is determined by the intercepts of the octahedral plane with the $\omega_1, \omega_2, \omega_3$ axes equation (3.2).

When \bar{X} is small, interactions between interstitials is reduced because the average separation δ between N atoms is large $\delta \sim a_0(2\bar{X})^{-1/3}$, for $\bar{X} < 0,025$, $\delta > 3a_0$.

When \bar{X} is close to $\frac{1}{8}$ the repulsive N-N interaction favors distributions showing NN a $\langle 111 \rangle$ doublets revealed by high hyperfine field on the Mössbauer spectra.

In order to describe the distribution of lattice deformations which varies inside domains λ^3 of coordinate $\vec{\chi}$ with a wave

length Λ it is proposed to utilise a multidimensional normal law : $p(\vec{\Omega})$.

This distribution integrates the fluctuation resulting from internal stress and of interstitial densities. It is possible to distinguish the influence of texture by choosing reference axes following the relation $\omega_1 \geq \omega_2 \geq \omega_3$.

According to the normal law any projection of $\vec{\Omega}$ obeys a normal law and if the mean of $\langle \vec{\Omega} \rangle$ is $\vec{\mu}$ and the second moment matrix $R = E \left[(\vec{\Omega} - \vec{\mu})(\vec{\Omega} - \vec{\mu})^T \right]$ the density function of $\vec{\Omega}$:

$$p(\vec{\Omega}) = \frac{1}{(2\pi)^{3/2} \sqrt{\det R}} \exp \left[-\frac{1}{2} (\vec{\Omega} - \vec{\mu})^T R^{-1} (\vec{\Omega} - \vec{\mu}) \right]$$

Because the distribution of $\vec{\Omega}$ does not show the same standard deviation along $\omega_1, \omega_2, \omega_3$ the distribution of interplanar distance will not be symmetrical and the diffraction peaks will be distorted and this could be a reason for the anomalous behaviour of a (θ) .

The continuous lattice distortion distributions which corresponds to the above described BM nitrogen alloying may present some analogy with those resulting from spinodal transformation likely to lead to diffraction difficult to decipher unambiguously, therefore the modelling of X-ray diffraction patterns based on interstitial distributions has not been achieved yet. Meanwhile this model corresponds to distortion platelets. The corresponding features are qualitatively consistent with the interpretation proposed by Aufrecht *et al* [6]. According to these authors the "anomalies" of the diffraction patterns observed with BM Fe N_x result from (112) stacking faults. This interpretation is also supported by High Resolution Transmission Microscopy (HRTEM) and molecular dynamics calculations.

Conclusions

Mössbauer characterized environments in B.M. carbides and nitrides are closely related with those of well crystallized structures. This similarity reveals a thermal short range reordering and concentration fluctuation taking place during the inter-impact periods of ageing. The need of cryogenic experiments likely to minimize thermally activated phenomena is underlined.

The role of planar defects such as stacking faults (6), distortion platelets consistent with diffraction and microscopy results as well as with computer simulation suggests the transfer of basic studies devoted to model interstitial alloys to industrial applications is likely to originate high performance steel grades especially in the case of multi-interstitial TRIP, TWIP, Bainitic Steels.

Acknowledgements

Experimental results as well as fruitful and pertinent discussions which support this lecture have been achieved thanks to

continuous collaborations with many colleagues and friends among whom: J. Aufrecht, Prof. Charlotte Becquart, Dr. Catherine Cordier, Dr. Le Caër, Dr. Leineweber, and Prof. E. Mittemeijer.

References

1. S.J. Campbell, H. Gleiter, Mössbauer effect studies of nanostructured materials. Long, J., Grandjean, F. (eds) *Mössbauer Spectrometry Applied to Magnetism and Materials Science*, 1, Plenum Press, New York, 1993, pp. 241-303.
2. E. Gaffet, G. Le Caër, Mechanical processing for nanomaterials. In: Nalwa H. S. (eds) *Encyclopedia of Nanoscience and Nanotechnology*, 5, American Scientific Publishers, 2004, pp. 91-129.
3. J. Foct, Mechano-synthesis of Fe₁₆N₂ from this special case to general principles, *Mater. Sci. Forum*, 325-326 (2000) 99-104.
4. J. Foct, G. Le Caër, Mechano-synthesis of interstitial compounds, *Ann. Chim. Sci. Mat.*, 22 (1997) 387-401.
5. J. Foct, C. Cordier-Robert, Ball milling induced interstitial atoms redistributions revealed by Mössbauer effect, *Hyperfine Interact.*, 190 (2009) 15-22.
6. J. Aufrecht, A. Leineweber, J. Foct, E. Mittemeijer; The structure of nitrogen-supersaturated ferrite produced by ball milling. *Phil. Mag.*, 88 (12) (2008) 1835-1855.
7. K.H. Jack, α -Fe₁₆N₂: a giant magnetic moment materials?. *Mater. Sci. Forum*, 325-326 (2000) 91-97.
8. P. Rochegude, J. Foct, The transformation $\epsilon \rightarrow \alpha'$ in iron-nitrogen solid solutions studies by Mössbauer spectrometry, *Phys. Stat. Sol. (a)*, 88 (1985) 137-142.
9. J.C. Rawers, D. Govier, R. Doan, Nitrogen addition to iron powder by mechanical alloying. *Mater. Sci. Eng.*, A220 (1996) 162-167.
10. J. Foct, An attempt to extract common behaviour from heterogeneous results about mechanical alloying. *J. Mat. Sci.*, 39 (2004) 5011-5017.
11. J.P. Morniroli, O. Richard, J. Foct, Study of the iron-nitrogen phases by electron microdiffraction and convergent beam electron diffraction, *Microsc. Microanal. Microstruct.*, 4 (1993) 575-594.
12. G. Le Caër, P. Delcroix, J. Foct, Contribution of Mössbauer spectrometry to the study of mechanically alloyed materials and of nanomaterials, *Mater. Sci. Forum*, 269-272 (1998) 409-418.
13. J. Foct, J.P. Senateur, J.M. Dubois, G. Le Caër, Mössbauer spectroscopy of different interstitial compounds and solid solutions containing ⁵⁷Fe. *J. Physique C2*, 3(40) (1979) 647-649.
14. C. Domain, C.S. Becquart, J. Foct, *Ab initio* study of foreign interstitial atom (C, N) interactions with intrinsic point defects in α -Fe, *Phys. Rev.*, B69, 144112 (2004) 1-16.
15. C.S. Becquart, C. Domain, J. Foct, *Ab initio* calculations of some atomic and point defect interactions involving C and N in Fe, *Phil. Mag.*, 85 (2005) 533-540.
16. J.P. Morniroli, E. Bauer-Grosse, M. Gantois, Crystalline defects in M₇C₃ carbides. *Phil Mag.* A48(1983) 311-327.
17. E. Bauer-Grosse, G. Le Caër, L. Fournes, Mössbauer study of amorphous and crystallized Fe_{1-x}C_x alloys, *Hyp. Int.*, 27 (1986) 297-300.